Pressure Drop in Oil Mist Filter Media: Validation of the Jump-and-Channel Model for a Broad Range of Air Velocities

H.E. Kolb*, J. Meyer and G. Kasper

Institut für Mechanische Verfahrenstechnik und Mechanik, Karlsruher Institut für Technologie,
76131 Karlsruhe, Germany

ABSTRACT

Experiments were made with glass microfiber media of the type used in oil mist filtration to test the jump and channel model by Kampa et al. (2014) across a range of typical filter face velocities (5 cm/s to 70 cm/s). The data show that the wet ∆p of an oleophilic filter is consistent with the model, in that the channel-∆p depends primarily on the loading rate, whereas a ∆p jump for a given medium does not depend on the operating conditions. The data also show that the so-called steady state mode of filter operation (i.e. at constant velocity and loading rate) is actually quasi-steady at best, and that the "steady-state" ∆p undergoes a gradual increase with time (termed "creep") that depends on operating conditions. Experimental data are also presented for the internal oil distribution in the channel flow region and an empirical model expression is developed for the internal global saturation (i.e. the average saturation within the channel region). Different models are explored for the dependence of ∆p on the internal oil distribution.

KEYWORDS

Filtration, coalescence filter, oil mist, pressure drop

Introduction

Submicron oil aerosols ("oil mist") are generated by a wide range of processes, such as metal cutting, engine crankcase ventilation, or the compression of gases. An efficient and commonly practiced way of capturing and removing oil mist is by fibrous filters. During steady-state operation of a mist filter, captured aerosol is driven by the airflow toward the rear surface of the media, where it drains as a thin film through which the air has to break through. Maintaining this steady-state flow of coalesced liquid requires an additional "wet ∆p" above and beyond the "dry ∆p" of the media. The wet ∆p of oleophilic filters is composed of an internal contribution ("channel-∆p") required to "pump" liquid through the media – typically in distinct channel-like structures – plus a final, steep "jump-∆p" required to overcome capillary retention forces and maintain the liquid drainage film on the surface. These mechanisms as well as their effect on the pressure drop of glass microfiber filter media are described by the "Jump-and-Channel" Model (Kampa et al., 2014) for a range of operating parameters. The validity and usefulness of the model is now extended to include a broader range of filtration velocities.

Experimental Materials and Methods

The oil mist used in this work was generated by a Collison-type nebulizer (May, 1973) in which dry compressed air disperses a typical compressor oil (surface tension 31 mN/m, dyn. viscosity 122 mPas) at room temperature and atmospheric pressure to sub-micron droplets with a mean diameter of about 300 nm. Further downstream this aerosol was mixed with a dry make-up flow to adjust the desired filtration velocity. Temperature and absolute pressure before the filter were monitored continuously. These inputs were used together with mass flow controllers to maintain the filtration velocity at a predetermined value in the range of 5 to 70 cm/s. By using up to three nebulizers in parallel the oil loading rate was varied between 15 and 125 mg/(s·m²). The rate of oil mass generation was kept constant by maintaining a constant Δp across the nebulizers throughout a run. The actual oil loading rate of the filter was determined on-line from the oil drainage rate. Aerosol penetration and oil re-entrainment were neglected in this calculation because the filters have overall efficiencies above 99.99% and entrainment was insignificant compared to the loading rate (Wurster et al., 2015).

The filters used is this study were built as “sandwiches” consisting of 10 identical, flat layers (thickness about 0.5 mm) of the same oleophilic glass microfiber media supported on the downstream side by a metallic grid support. The weight per unit area of each filter layer was measured before clamping the sandwich in a metal frame and installing it vertically in the filter unit. Each run started with a fresh, dry sandwich that was loaded under exactly constant conditions for several hours past reaching steady-state operation. (For oil mist filters, steady state is commonly defined as operation at a constant drainage rate and pressure drop. Note however, that some filter media under certain operating conditions exhibited a kind of “Δp-creep”, which will be addressed later

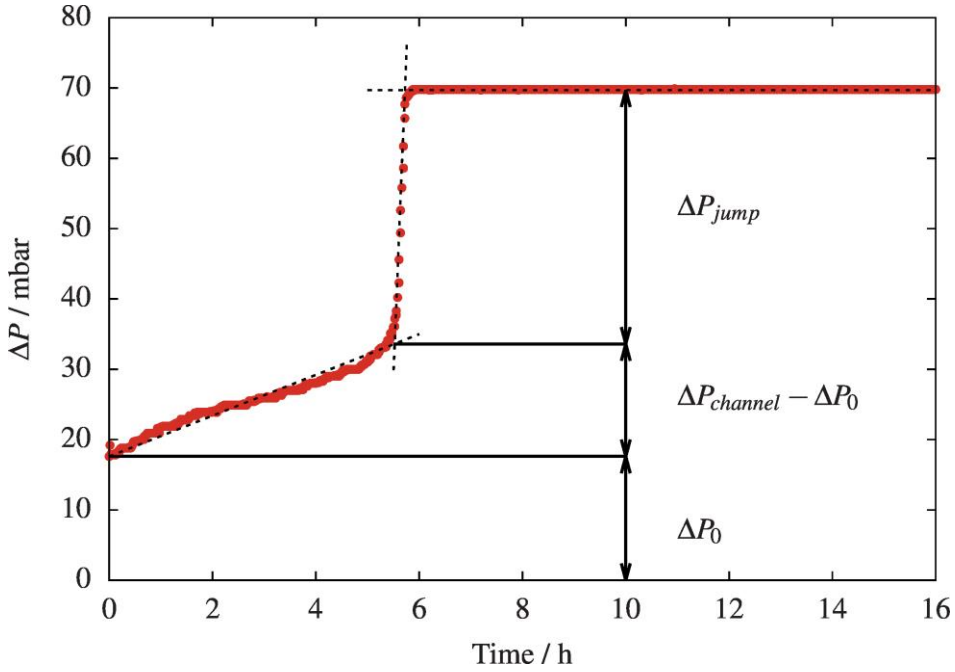

Fig. 1 – *Graphical method to determine the characteristic pressure drop components channel-Δp and jump-Δp*

in this paper.) At the end of a run, the sandwich was immediately taken apart to photograph each layer for the purpose of image analysis of the oil channel distribution, and/or to measure the oil content.

The mean saturation per layer was determined gravimetrically after removing about 5 mm of the edges where the media had been clamped in the filter mount. Photographs were taken of each layer, converted to black & white images via a pre-determined threshold of gray level, and evaluated by automated image analysis for the local oil distribution, especially the size and number of oil channels. This threshold was determined in such a manner that the gravimetrically measured saturation matched the area-equivalent saturation of the image analysis.

The temporal evolution of Δp during the start-up phase of a filter was analyzed and broken down into its basic constituents according to the Jump-and-Channel Model by a graphical method first suggested by Kampa et al. (2014). For the case of an oleophilic filter, this method divides the Δp-curve into three quasi-linear sections as seen in Fig. 1. The first section is due to the formation of oil channels. The slope of this channel-Δp region is usually quite modest when compared to the following, steep increase caused by the formation of an oil film on the rear face of the filter. This film, which is quasi-continuous and maintained on the surface by the gas flow, acts as the drainage flow. The last section of the Δp-curve is what we call steady state, i.e. with constant drainage, a constant internal oil distribution, and (supposedly) no further changes in Δp. The linearized slopes for the channel-Δp and the Δp-jump are obtained from the intersections of the respective tangents as indicated in Fig. 1.

Results: (1) Dependence of pressure drop on operating parameters

Experiments were carried out for face velocities of 5, 10, 25, 40 and 70 cm/s at nominal oil loading rates of 15, 60 and 125 g/(s·m²), giving a set of 15 combinations, not counting repeated runs, and taking over 6 months to complete. A representative set of data for one fixed velocity of 25 cm/s is shown in Fig. 2. As expected from our model, the slope of the channel-Δp section becomes steeper with increasing oil loading rate, and also shifts the steady-state Δp to higher values. The height of the Δp-jump however, remains constant.

For constant v, this type of behavior was already described by Kampa et al. (2015), who explained it with capillarity for the jump vs. energy considerations for the channels: The Δp-jump is determined primarily by the media structure and the surface tension. It should thus be independent of loading rate and flow velocity. Conversely, the channel-Δp is the result of oil transport and increases with loading rates, because more oil has to be pumped per unit time. On the other hand, it should not depend on the flow velocity.

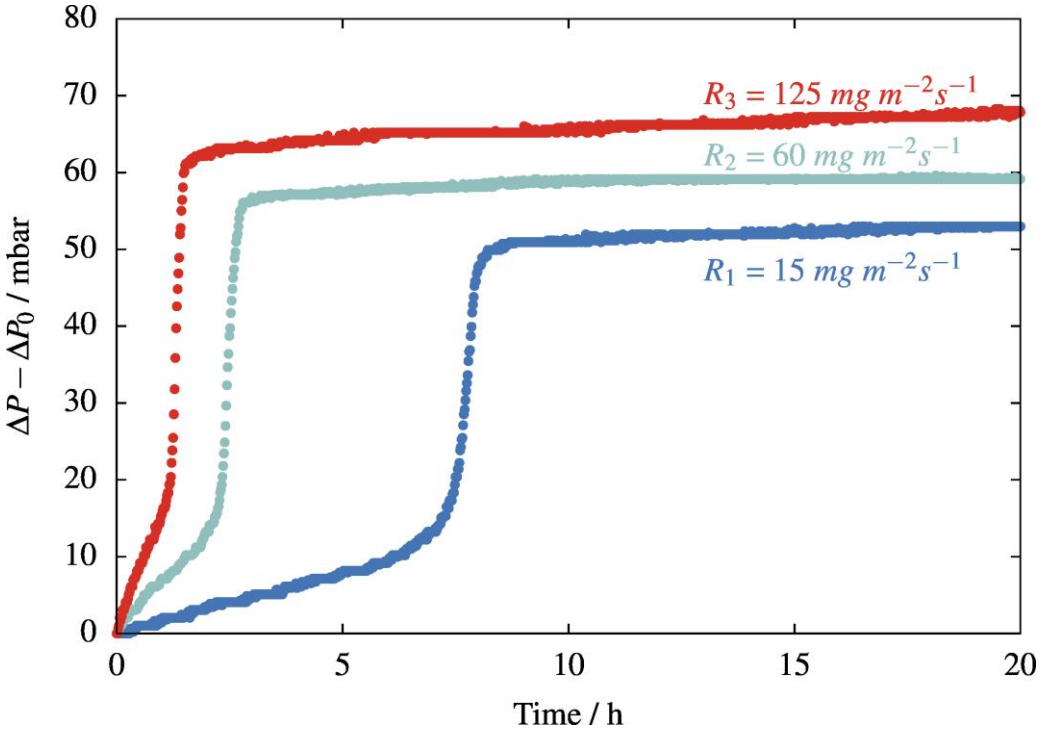

Fig. 2 – *Δp vs. time for different loading rates at a constant velocity of 25 cm/s*

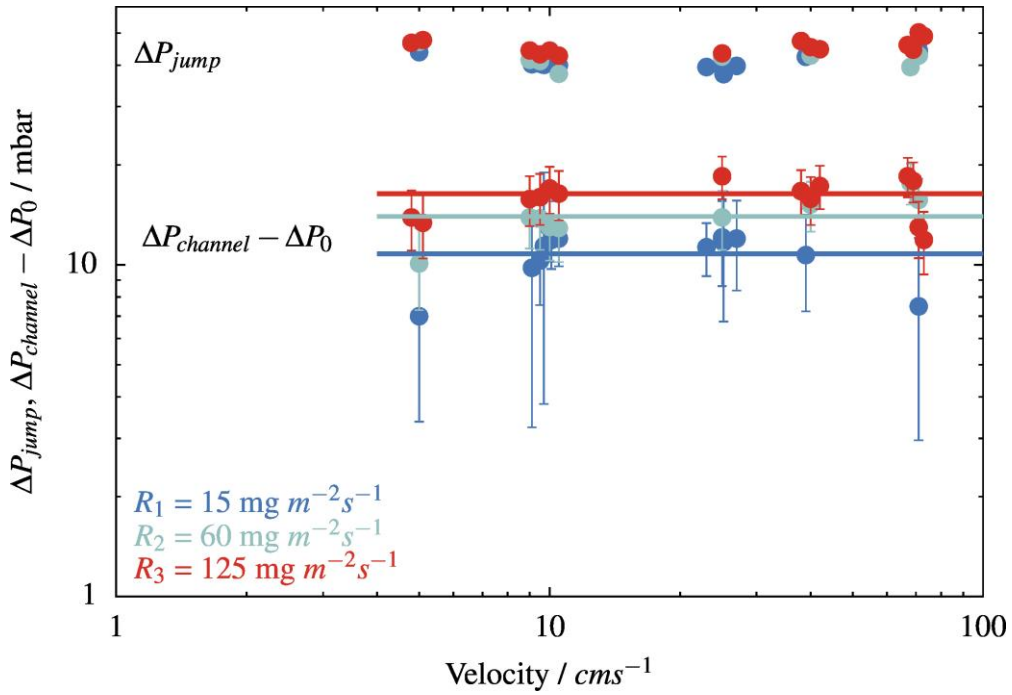

Fig. 3 – *Measured jump-Δp and channel-Δp vs. airflow velocities of 5, 10, 25, 40 and 70 cm/s for different oil loading rates (points for constant velocities are displaced sideways). Horizontal lines of the channel-Δp represent averages for each loading rate.*

In Fig. 3 we are able to show that the Δp-jump is indeed constant for all our combinations of operating parameters. In particular we see no systematic dependence on loading rate or filtration velocity within the accuracy and reproducibility of our experiments. The influence of operating parameters on the channel-Δp is harder to discern visually from Fig. 3, because there is more variability in the data for several reasons addressed below. Averaging these values (the horizontal lines in Fig. 3) shows however that there is a systematic increase with oil loading rate, while regression analyses show no significant variation with flow velocity. The assumptions of our model thus seem to hold true for a wide range of operating conditions.

The channel-Δp data are more noisy because their absolute level is quite low (7 to 20 mbar) and therefore susceptible to errors from various sources. For one, there is some variability in the oil loading rate, which has a direct impact on Δp. This variability does not arise from fluctuations during a given run (which were very small) but between runs, possibly from small seasonal variations in ambient temperature (and thus in oil viscosity) and other factors (such as aerosol losses upstream of the filter) which impacted the oil delivery rate at the front face of the filter by as much as $\pm$5 mg/(s·m²). (The exact oil delivery rate could be determined only after an experiment from the drainage rate.) Other reasons for experimental uncertainty include the accuracy of the pressure transducer ($\pm$1 mbar), the graphical method ($\pm$1 mbar), which affect the channel-Δp more strongly because its absolute level is very low. The impact of those effects on the channel-Δp is estimated by the error bars in Fig. 3. Last but not least there is the inhomogeneity of the filter media, as evidenced by variations in dry pressure drop up to 30 % (for the smaller velocities) from sandwich to sandwich. Presumably this affected the channel structure, the channel-Δp and caused some variation in the Δp jump as well.

Results: (2) Parameter dependence of global saturation and internal oil distribution

The liquid saturation in mist filters is typically expressed as a global value for the entire filter (Liew and Conder, 1985; Frising et al., 2005; Mead-Hunter et al., 2013). Earlier work by Kampa et al. (2015), as well as our own current results indicate, however, that it varies systematically within a sandwich in the direction of flow. The saturation typically starts rather high with up to 50% in the front-most layers, due to coalescence of deposited droplets and a subsequent formation of the oil-channels which takes place in the first one or two layers. It then drops and levels off to a constant value in the midsection of the filter where the channels are well developed. The last layer of an oleophilic sandwich always shows an increased saturation due to imbibition of the oil film when the airflow is shut off. This film causes the Δp-jump and must be regarded as an external film during operation.

To avoid this artifact, we exclude layer 10 from the determination of the global saturation and base it on the average of layers 1 to 9. Fig. 4 shows that the saturation increases

systematically with the oil loading rate but decreases with velocity. (The slight up-swing at 70 cm/s is due to another reason, namely massive Δp-creep, which will be addressed later.) Both behaviors are logical consequences of the jump-and-channel model, which suggests that additional Δp ("wet Δp") is required to pump oil through the filter. Higher oil loading rates thus require more pressure drop. This additional Δp can be generated inside the filter, either by increasing the saturation (in case of constant v), or by increasing v. In case of a constant loading rate, the saturation thus goes down as the flow velocity goes up.

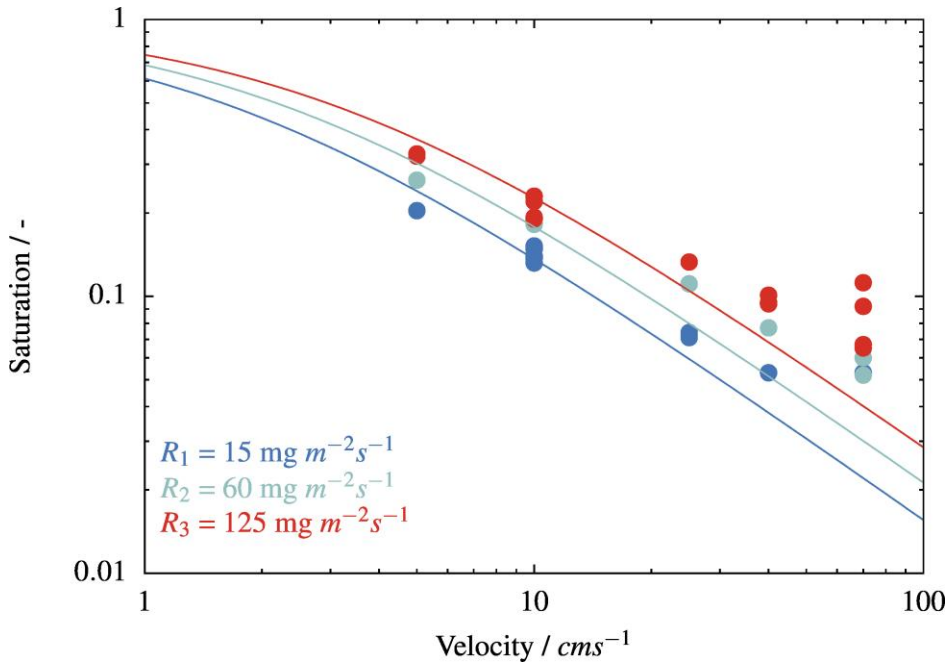

Fig. 4 – *Measured "internal" saturation and calculated saturation (using Eq. 1 and Tab. 1) vs. airflow velocity for different oil loading rates*

A systematic decrease in saturation with airflow velocity has been reported earlier (Mead-Hunter at al., 2013) for pre-saturated or "dipped" glass microfiber media that were challenged with a constant oil loading rate at filtration velocities of 30 cm/s or less. (These authors included the imbibed film on the downstream filter face, which makes values a harder to compare values for S.) Based on their observations, the authors suggested a linear proportionality of the type $S = -A\ v + B$ where B depends on the number of layers in the sandwich. We have adapted this expression for our purposes in the following way to model the average saturation for an arbitrary number of layers

$$S = \frac{1}{1 + \frac{v}{v_{char}}}$$

Eq. (1)

Eq. (1) is bounded by 0 and 1 for very high and very low flow velocities, respectively. v_{char} is a characteristic velocity that depends on media structure and oil loading rate. v_{char} was determined for each loading rate by fitting the above expression to our data, as seen in Table 1:

Oil loading rate / mg/(s·m²)	v_{char} / cm/s
15	1.58
60	2.17
125	2.93

Tab. 1 – *Characteristic velocities for different oil loading rates*

Global saturation does not take into account the existence of oil channels or any other aspects of internal oil distribution in a mist filter, either in flow direction or within the plane of the filter. Nevertheless it remains an indispensable parameter to describe the state of operation of mist filters, last but not least because it can be determined very accurately and with relative ease. We have used it to investigate the dependence of oil channel geometry on filter operating parameters (Fig. 5). The number and mean projected area equivalent diameter of oil channels was determined by image analysis from photographs of the individual layers. Since there is some uncertainty in practice, in determining the exact edge of the channels by such a method, we have used the gravimetric saturation as a calibration in setting the contrast threshold for image analysis.

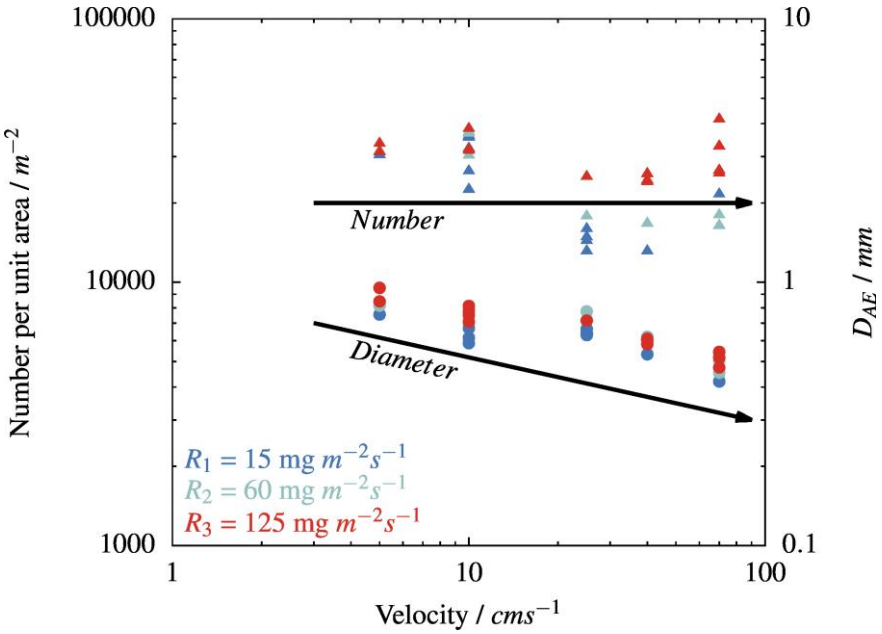

Fig. 5 – *Channel number and diameter vs. airflow velocity for different oil loading rates*

Despite considerable experimental noise in the data on number and size of oil channels, Fig. 5 shows that the number of channels per unit filter area is roughly independent of

flow velocity, but that their size decreases. Since the global saturation also decreases with flow velocity, this behavior suggests that the transport velocity of the oil must increase with the airflow velocity. With regard to an increase in oil loading rate, the system tends to respond preferentially by creating additional oil channels. The analysis leading to Fig. 5 assumes that oil channels are fully saturated in an otherwise dry filter. However, visual observation indicates the existence of partially wetted region within the filter, presumably because oil transport within the channels occurs discontinuously, drop by drop. Hence, there are two limiting cases for the internal oil distribution, which directly impact the dependence of Δp on S. In case of oil flow in fully saturated channels vs. airflow in completely dry regions, the wet Δp in the channel region is related to the dry Δp_0 simply by the increase in internal flow velocity:

$$\frac{\Delta P_{channel}}{\Delta P_0} = \frac{1}{(1-S)} \qquad \text{Eq. (2)}$$

In the other limit, one could envisage a perfectly homogeneous oil distribution with no oil channel structure at all, where liquid would have to form a uniform film on the fibers. The rise of the channel-Δp with S would then occur via an increase in fiber diameter d_f as well as the change in porosity ε. Based on well-known models for the pressure drop in porous media, the increase in Δp would thus behave in the following way:

$$\frac{\Delta P_{channel}}{\Delta P_0} = \frac{\frac{1-\varepsilon_{eff}}{\varepsilon_{eff}^4}}{\frac{1-\varepsilon_0}{\varepsilon_0^4}} \left(\frac{d_f}{d_{f,0}}\right)^2 = \frac{1}{(1-S)^4} \qquad \text{Eq. (3)}$$

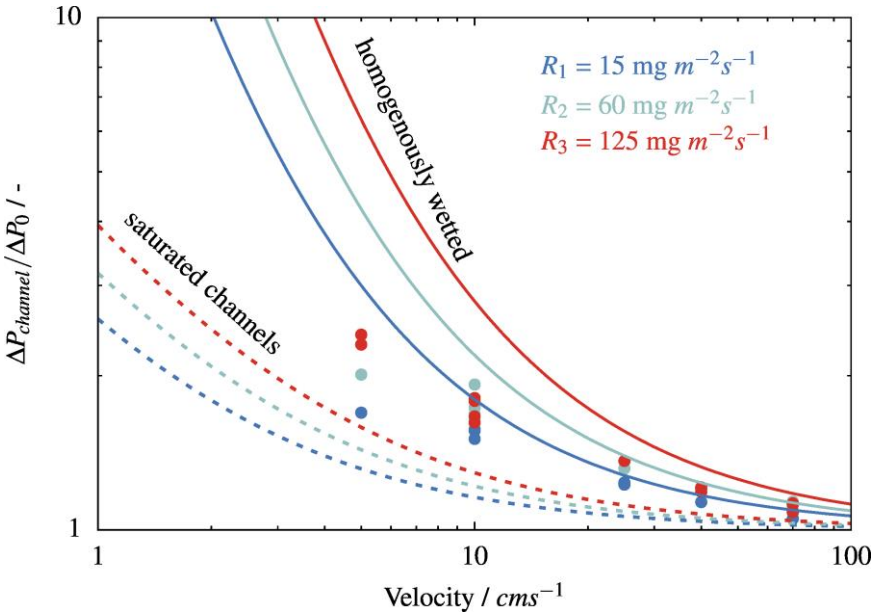

Fig. 6 – *Relative increase of channel-Δp with airflow velocity: Comparison of measurements with theoretical limiting cases of internal liquid distributions Eq.2 and 3.*

In Fig. 6 we compare the actual dependence of $\Delta P_{channel}/\Delta P_0$ on flow velocity with the two limiting model cases, using Eq. (1) and Table 1 to calculate $S(v)$. Obviously, the actual liquid distribution in the filter does not correspond too well to either of the two extreme possibilities, which nevertheless provide brackets for the range for the possible internal ∆p. It also becomes clear that the formation of channels contributes significantly to the reduction the wet ∆p!

Results: (3) Pressure drop creep during quasi-steady operation

It is usually assumed that the ∆p of a mist filter remains constant once it operates in steady state (e.g. Frising et al., 2005; Gac, 2015; Mead-Hunter et al., 2014; Kampa et al., 2015). Such an assumption entails a constant global saturation as well as a constant oil distribution within the filter. However, our database clearly shows that ∆p is indeed not really constant but increases systematically, although often very slowly – hence the term “creep” – even though the operating conditions are kept very constant. Moreover, creep seems to go on quasi indefinitely in time. Many quasi-steady states observed during this study had an increase of no more than 2% within 20 hours (the usual duration of our runs), but some experiments showed a much more significant increase of their ∆p. Fig. 7 presents a typical data set for different airflow velocities at one constant loading rate. It shows that experiments at higher airflow velocities are prone to such a ∆p-creep, whereas smaller velocities result in a more constant ∆p during the time of observation. Similar phenomena can also be observed in the data presented by the above-mentioned papers, but so far the phenomenon has never been mentioned explicitly in the literature. Our investigations show that creep is associated with a slow increase in saturation. (This also explains why some saturation values in Fig. 4 for a flow velocity of 70 cm/s were overestimated.) Creep is currently a subject of more detailed investigations.

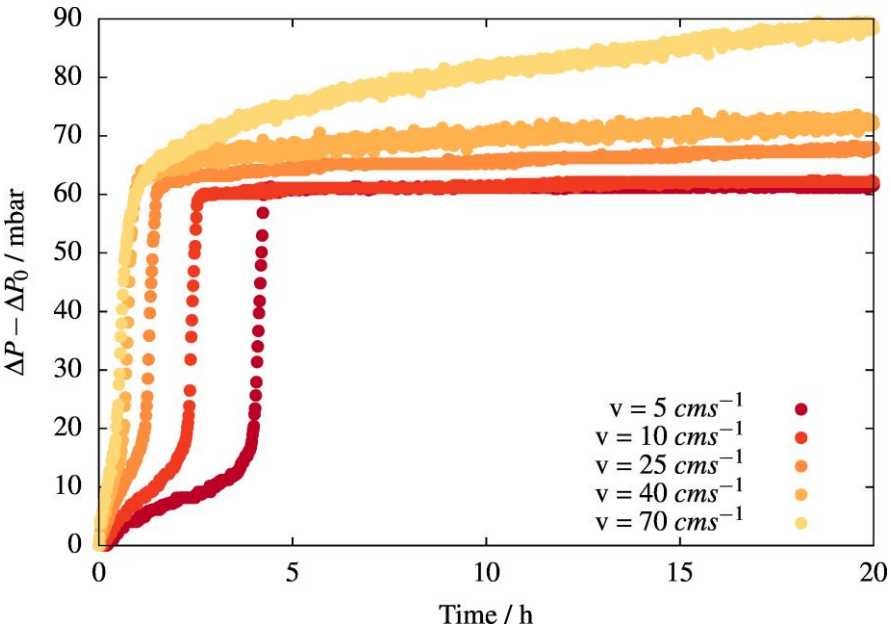

Fig. 7 – *Δp vs. loading time for the same filter medium at five different airflow velocities and a constant oil loading rate. Δp-creep can be observed for airflow velocities of 25, 40 and 70 cm/s.*

Conclusions

Experiments were made with glass microfiber media of the type used in oil mist filtration to test the jump and channel model by Kampa et al. (2014) across a range of typical filter face velocities (5 cm/s to 70 cm/s). The data show that the wet Δp of an oleophilic filter is consistent with the model, in that the channel-Δp depends primarily on the loading rate, whereas a Δp jump for a given medium does not depend on the operating conditions.

Experiments show that the so-called steady state mode of filter operation is indeed quasi-steady at best, and that Δp undergoes a gradual increase with time (termed “creep”) that depends on operating conditions.

Experimental data are presented for the internal oil distribution in the channel flow region and an empirical model expression is developed for the internal global saturation (i.e. the average saturation within the channel region). Different models are explored for the dependence of Δp on the internal oil distribution.

References

Frising, T., Thomas, D., Bémer, D., Contal, P., 2005. Clogging of fibrous filters by liquid aerosol particles: Experimental and phenomenological modelling study, Chem. Eng. Sci. 60, pp. 2751-2762.

Gac, J.M., 2015. A Simple Numerical Model of Pressure Drop Dynamics During the Filtration of Liquid Aerosols on Fibrous Filters. Sep.Sci. Technol. 50, pp. 2015-2022.

Kampa, D., Wurster, S., Buzengeiger, J., Meyer, J., Kasper, G., 2014. Pressure drop and liquid transport through coalescence filter media used for oil mist filtration. Int. J. Multiphase Flow. 58, pp. 313-324.

Kampa, D., Wurster, S., Meyer, J., Kasper, G., 2015. Validation of a new phenomenological “jump-and-channel” model for the wet pressure drop of oil mist filters. Chem. Eng. Sci. 122, pp. 150-160.

Liew, T.P., Conder, J.R., 1985. Fine mist filtration by wet filters – I. Liquid saturation and flow resistance of fibrous filters, J. Aerosol Sci. 16, pp. 497-509.

May, K.R., 1973. The Collison Nebulizer: Description, Performance and Application. Aerosol Sci. 4, pp. 235-243.

Mead-Hunter, R., Braddock, R.D., Kampa, D., Merkel, N.,Kasper, G., Mullins, B.J. 2013. The relationship between pressure drop and liquid saturation in oil-mist filters – Predicting filter saturation using a capillary based model. Sep. Purif. Technol. 104, pp. 121-129.

Wurster, S., Kampa, D., Meyer, J., Müller, T., Mullins, B. J. and Kasper, G., 2015. Measurement of oil entrainment rates and drop size spectra from coalescence filter media, Chem. Eng. Sci. 132, pp. 72-80.